

NJC

Accepted Manuscript



This is an *Accepted Manuscript*, which has been through the Royal Society of Chemistry peer review process and has been accepted for publication.

Accepted Manuscripts are published online shortly after acceptance, before technical editing, formatting and proof reading. Using this free service, authors can make their results available to the community, in citable form, before we publish the edited article. We will replace this *Accepted Manuscript* with the edited and formatted *Advance Article* as soon as it is available.

You can find more information about *Accepted Manuscripts* in the [Information for Authors](#).

Please note that technical editing may introduce minor changes to the text and/or graphics, which may alter content. The journal's standard [Terms & Conditions](#) and the [Ethical guidelines](#) still apply. In no event shall the Royal Society of Chemistry be held responsible for any errors or omissions in this *Accepted Manuscript* or any consequences arising from the use of any information it contains.



www.rsc.org/njc

Cite this: DOI: 10.1039/c0xx00000x

www.rsc.org/xxxxxx

ARTICLE TYPE

Facile synthetic route to convert Tb(III) complexes of novel tetra-1,3-diketone calix[4]resorcinarene into hydrophilic luminescent colloids

Nataliya A. Shamsutdinova,^a Sergey N. Podyachev,^a Svetlana N. Sudakova,^a Asiya R. Mustafina,^a Rustem R. Zairov,^{*a} Vladimir A. Burilov,^b Irek R. Nizameev,^a Ildar Kh. Rizvanov,^a Victor V. Syakaev,^a Bulat M. Gabidullin,^a Sergey A. Katsuba,^a Aidar T. Gubaidullin,^a Georgy M. Safiullin^c, and Wim Dehaen^d

Received (in XXX, XXX) Xth XXXXXXXXX 20XX, Accepted Xth XXXXXXXXX 20XX

DOI: 10.1039/b000000x

The work represents the synthesis of a novel calix[4]resorcinarene cavitand bearing four 1,3-diketone groups at the upper rim and its complex formation with Tb(III) ions in DMF and DMSO solutions.

Electrospray ionization mass spectrometry, ¹H NMR, UV-Vis and luminescence spectra indicate a long (three hours at least) equilibration time of the complex formation between the cavitand and Tb(III) in alkaline DMF and DMSO solutions. These results are explained by the restricted keto-enol conversion, resulting from the steric hindrance effect of the methylenedioxy-groups linking the benzene rings within the cavitand framework. A facile synthetic route to convert luminescent Tb(III) complexes of various stoichiometry into luminescent hydrophilic colloids is disclosed in this work. The route is based on the reprecipitation of the Tb(III) complexes from DMF to aqueous solutions with further polyelectrolyte deposition without prior separation of the luminescent complexes. The luminescent colloids exhibit high stability over time and in buffer systems, which is a prerequisite for their applicability for analysis and biolabeling.

Introduction

The development of bioresponsive luminescent lanthanide complexes has experienced major advances in past decades.¹⁻⁷ The high sensitivity and fast time of optical imaging make these lanthanide complexes ideal for the detection of analytes in the low concentration range. The origin of the substrate induced luminescent response is based on the energy transfer phenomenon.⁵⁻⁸ It is worth noting that ternary complex formation is of particular impact in the development of the substrate induced luminescence response. Luminescent lanthanide complexes with 1,3-diketones due to their incomplete coordination sphere are able to bind various organic substrates because of ternary complex formation, which in turn has been successfully applied in sensing and imaging.⁸⁻¹⁴ Moreover 1,3-diketone derivatives with fluoro-aliphatic and aromatic substituents are of particular interest due to their significant antennae effect on lanthanide-centered luminescence.¹⁵⁻¹⁶ Calix[4]arene and calix[4]resorcinarene scaffolds with four phenol or resorcinol units are of significant impact in the development of novel ligands for lanthanides.¹⁷⁻²⁰ The Tb(III) complex with p-sulfonatocalix[4]arene should be mentioned as a fine example of a highly luminescent water soluble complex,¹⁹⁻²¹ which nevertheless should be protected or encapsulated into some polymeric matrix to be applied for marking and sensing.^{22,23} Indeed, calixarene based lanthanide complexes, which combine water solubility, enhanced antennae

effect on lanthanide-centered luminescence and high stability in aqueous buffer solutions are very rare if existent at all.

The application of luminescent lanthanide complexes with 1,3-diketones in sensing is restricted to a larger extent by their poor solubility in aqueous solutions, since the sensing in organic solutions significantly complicates the sample preparation protocols. The doping of water insoluble lanthanide complexes into nanoparticles with their further hydrophilic coating is a promising alternative to a covalent modification of ligands with ionic groups as a route to improve water solubility.^{1,6,22-26} Moreover, the core-shell morphology of nanoparticles leads to a route to gain biocompatibility by encapsulation of hazardous luminophores into a biocompatible polymeric matrix, which affords a biomedical application of the nanoparticles. Although silica coating is a well developed route to make core-shell nanoparticles, including those with lanthanide-centered luminescence, its shortcomings are worth noting. The synthetic conditions, which have been applied for the hydrolysis of tetraethoxysilane, in particular the use of highly alkaline aqueous or alcohol solutions, result in definite requirements to solubility and stability of luminescent complexes doped into silica nanoparticles.²² The previously reported approach²⁷ enables to dope Eu(III) complexes into the core of nanoparticles through the reprecipitation from organic to aqueous solutions with further colloid stabilization by means of polyelectrolyte layer-by-layer deposition. These colloids are stable for at least a week, without detectable degradation of their luminescence, while the silica nanoparticles doped with the same complex through the Stober

procedure suffer from instability of the Eu(III) centered luminescence.²⁸ Moreover, our previous results reveal the similarity between the luminescent response of Eu(TTA)₃-based complexes both in organic solvents and in aqueous dispersions of Eu(III) polyelectrolyte deposited nanoparticles.²⁹ Nevertheless the previously reported colloids suffer from partial degradation in concentrated phosphate and citrate buffer solutions, which restricts their applicability in biosensing.

The present work introduces a novel calix[4]resorcinarene cavitand with four *1,3*-diketone groups at the upper rim (**4** in the Scheme 1), its complex formation with Tb(III) ions and the efficient antennae effect on Tb(III) centered luminescence. The polyelectrolyte layer-by-layer deposition technique was successfully applied in this work as a facile synthetic approach to go from Tb(III) complexes of **4** to hydrophilic core-shell nanoparticles exhibiting a high stability of colloid and luminescent properties.

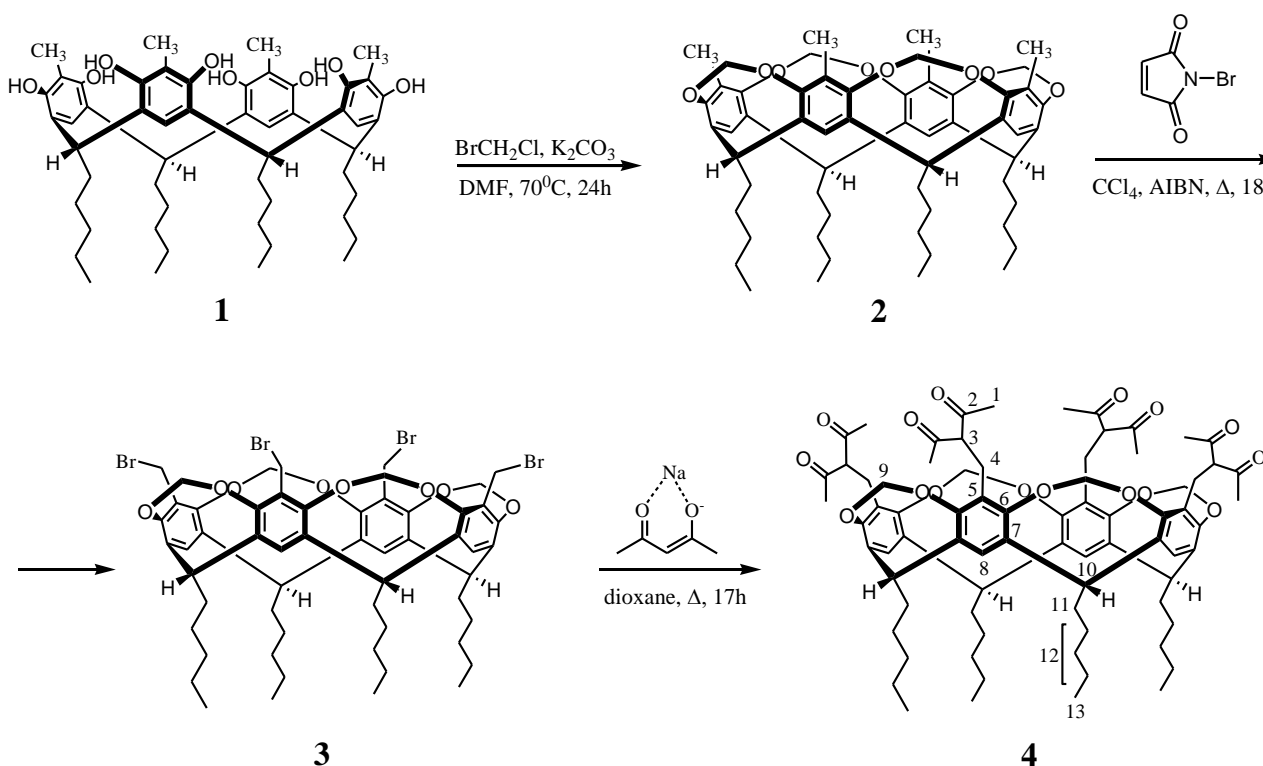
Results and discussion

Synthesis and characterization of 7,11,15,28-tetrakis[(acetylaceton-3-yl)methyl] calix[4]resorcinarene cavitand **4**

The Claisen condensation is a common synthetic strategy for *1,3*-

diketones, although it is unsuccessful in the synthesis of poly-*1,3*-diketone derivatives due to competitive reactions, such as aldol and ester condensations and some others. The condensation of ketones with acyl chlorides instead of esters, the use of protective groups and the nucleophilic substitution of alkyl halides with *1,3*-diketones can be listed as more convenient synthetic routes to obtain both diketone and polydiketone derivatives.³⁰⁻³² The latter synthetic route was successfully applied to embed two *1,3*-diketone groups to the calix[4]arene upper rim.³³ The nucleophilic substitution of *1,3,5*-tris(bromomethyl)benzene with *1,3*-diketone sodium salts was successfully applied in our previous work introducing the synthesis of the mesitylene derivative substituted by three *1,3*-diketone moieties.³⁴ A similar approach to incorporate four *1,3*-diketone groups to the upper rim of calix[4]resorcinarene cavitand is introduced herein.

The Scheme 1 represents the synthetic route for **4** with the introduction of the synthesis of some earlier reported intermediates. The known tetrakis(bromomethyl)cavitand **3** was stirred and refluxed with the sodium salt of acetylaceton in dioxane to give **4** (63%). The obtained compound was characterized by the combination of NMR, IR and MS techniques (See Fig. S1-S3 in ESI). The 3D structure of **4** was finally established by single crystal X-ray crystallography.



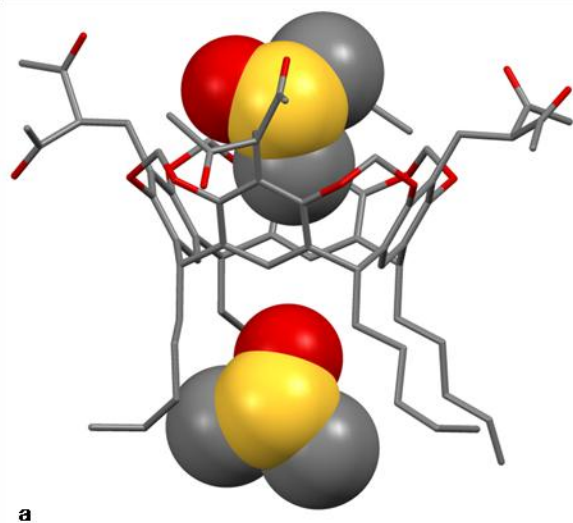
Scheme 1 Synthetic routes and structural formulae of the compounds **1-4**. The similar numbering system of atoms is used in the experimental section.

For tetrakis[(acetylaceton-3-yl)methyl] calix[4]resorcinarene cavitand **4** the bands assigned to the $\nu(\text{C}=\text{O})$ vibrations are revealed at 1725 and 1701 cm^{-1} (Fig. S3, ESI). The doublet character of the keto-carbonyl bands derives from syn- and antiphase stretching vibrations of the carbonyl groups in the *1,3*-diketone fragments.³⁵

The keto-enol tautomerism of *1,3*-diketones is influenced by

synergistic interplay between π -delocalization and H-bond strengthening.³⁶ Earlier literature³⁷⁻³⁹ highlights the impact of the substituents in tuning the hydrogen bond strength of *1,3*-diketones in solvents of diverse polarity. The comparison of the keto:enol ratio for two structurally analogous tris-*1,3*-diketones, namely tris(acetylaceton) γ -carbon-linked to mesitylene³⁴ and tris(methyl)mesitylene⁴⁰ spacers reveals significant difference

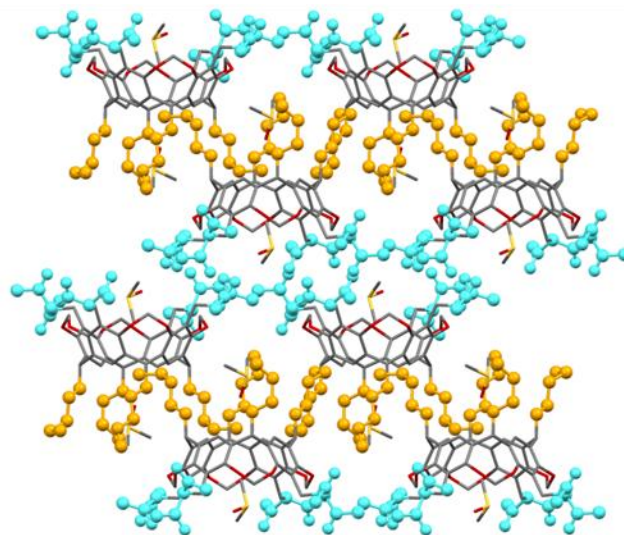
between them. Indeed, the percentage of the enolic form is significant for the former (~35%),³⁴ while it amounts to nothing for the tris(methyl)mesitylene based tris-*1,3*-diketone in CDCl₃ solutions.⁴¹ This difference confirms the effect of the steric hindrances induced by the methyl groups adjacent to *1,3*-diketone moieties on the stabilization of the enolic forms of these derivatives. The structure of **4** (Scheme 1) reveals that each *1,3*-diketone group is in proximity with the methylenedioxy substituents linking the cavitand scaffold. Taking into account the difference in keto-enol transformations for tris-*1,3*-diketones with mesitylene³⁶ and tris(methyl)mesitylene⁴² spacers, a restricted keto-enol transformation may be anticipated for **4**. The ¹H NMR spectra of **4** in CDCl₃ indicate an insignificant fraction of the enolic form (no more than 5-10%), which confirms the above mentioned assumption about the steric hindrance of the methylenedioxy substituents.



a

The structure revealed from X-ray data confirms that cavitand **4** adopts a "cone" conformation with a close to identical arrangement of the side aromatic rings relative to a reference plane passing through the four bridging carbon atoms. The asymmetric unit of the unit cell contains the cavitand molecule with two DMSO molecules embedded into its upper and lower pseudo-cavities (**4**·2DMSO, Fig. 1a). The analysis shows the disorder of both DMSO molecules and of the alkyl moieties of **4** over two positions. It is worth noting that the four *1,3*-diketone fragments exist in the keto form and point out of the cavity.

The molecules of **4** lack of classical hydrogen bond donor groups. Thus the primary supramolecular motif in the crystals of **4**·2DMSO is based on non-classical C-H...O type hydrogen bonds. The packaging of the molecules results in the formation of a layered structure of alternating (semi-)hydrophilic and hydrophobic sheets (Fig. 1b).



b

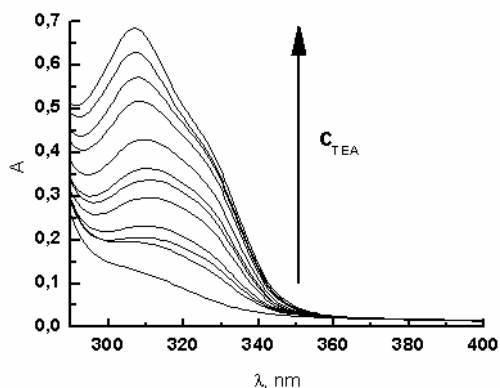
Fig. 1 (a) Molecule of **4** with two DMSO molecules represented in space-filled model. Hydrogen atoms are omitted for clarity. All disordered molecules and fragments are shown at the positions with greater occupancies. (b) Supramolecular packaging in the stick representation; viewed along the Ox crystallographic axis. Hydrophobic alkyl moieties are shown as orange balls and hydrophilic *1,3*-diketone groups - as blue balls.

Complex formation of **4** with Tb(III) in solutions

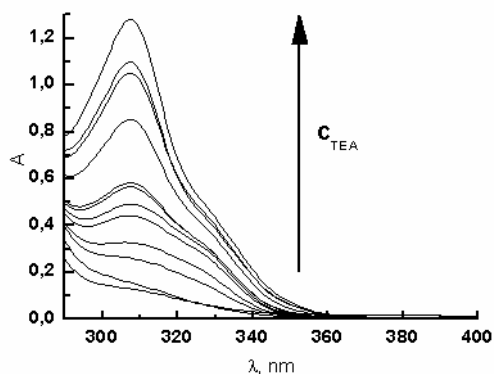
The presence of four *1,3*-diketone groups at the upper rim of cavitand **4** is the prerequisite of its complex formation with lanthanides in alkaline conditions. Cavitand **4** is well soluble in DMSO and DMF, while its solubility is poor in alcohols. The solubility of **4** is enhanced in alkaline conditions, which can be exemplified by the dissolution of **4** in chloroform-methanol mixture in the presence of a four-fold excess of triethylamine (TEA). The addition of Tb(III) nitrate to this solution results in the precipitation (the procedure is presented in more detail in the ESI). The elemental analysis data (presented in the ESI) reveal the effect of the Tb:**4** concentration ratio on the composition of the precipitates. Moreover the elemental analysis data can not be assigned to any definite stoichiometry, which indicates the co-occurrence of complexes with diverse stoichiometry. The convenient solubility of both **4** and its lanthanide complexes

in DMSO and DMF explains their choice as solvents to study the complex formation with Tb(III) ions by both UV-Vis, electrospray ionization mass spectrometry and ¹H NMR spectroscopy. The complex formation of **4** with Tb(III) ions is accompanied by the deprotonation of the *1,3*-diketone moieties to diketonates, which results in an increase of electronic absorption between 300-350 nm in the UV-Vis spectra of **4** (Fig. 2) upon the addition of TEA to solutions of **4** and Tb(NO₃)₃. The data in Fig.2 exemplify that the spectral changes in DMSO solutions at 1:1 (Tb:**4**) concentration ratio upon the addition of diverse amounts of TEA tend to increase in time (the spectra recorded in DMF reveal the similar trend).

A Job plot analysis of the spectral measurements with a varied Tb:**4** molar ratio and a 1:4 **4**:TEA molar ratio in DMF solutions was performed with different time intervals between the preparation of the solutions and their measuring.



a



b

Fig. 2 UV-Vis spectra of **4** (0.1 mM) in the presence of Tb(III) ions (0.1 mM) under the varied concentration of TEA (0.05-1.2 mM) within 10 minutes after the samples preparation (a) and after one day of their storage (b).

5 The profile of the Job plot tends to change in time, which indicates a time dependent complex formation (Fig. 3). The spectral changes are most significant within one day (Fig. 3a,b,c), while no further significant changes are observed after three days storage of the solutions (Fig. 3d). The electrospray (ESI)

10 ionization mass spectra recorded for recently (within one hour) prepared DMF solutions of **4**, Tb(III) and TEA in 1:1:4 (Tb:4:TEA) concentration ratio (Fig. 4) reveal the peaks corresponding to two positively charged 1:1 complexes. The major peak at m/z^{++} 747.9 (Fig.4a) corresponds to a doubly charged 1:1 complex with Tb(III) ion coordinated with one 1,3-diketonate group and one DMF molecule ($[\text{Tb}^{3+}\text{DMF}][\mathbf{4}^-]$). The peak at m/z^+ 1494.7, corresponding to a 1:1 positively charged complex, where the Tb(III) ion is coordinated with two enolate groups and one DMF molecule ($[\text{Tb}^{3+}\text{DMF}][\mathbf{4}^{2-}]$), is present to a minor extent (Fig. 4a). One day storage of this solution results in significant lowering of the peak at m/z^{++} 747.9 and the appearance of a peak corresponding to a doubly charged 2:1 complex (m/z^{++} 862.3), which results from the coordination of two Tb(III) ions with four diketonate groups and two DMF molecules ($[\text{Tb}^{3+}\text{DMF}]_2[\mathbf{4}^{4-}]$) (Fig.4b).

25

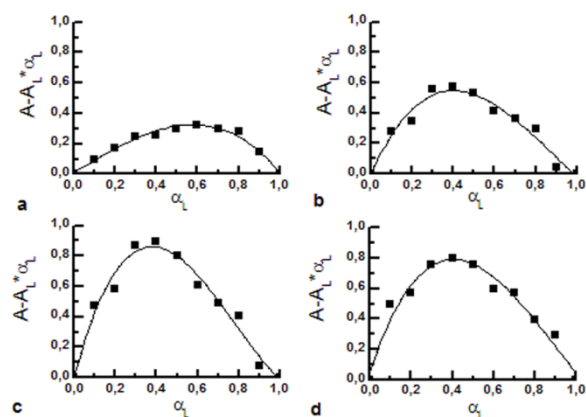


Fig. 3 The Job plot profiles for the DMF solutions at varied Tb:4 molar ratio ($[\text{Tb}]+[\mathbf{4}]=0.2$ mM) and 4:TEA concentration ratio remaining at the 1:4 level for the recently (within 10 minutes) prepared solutions (a) and under various time of their storage: 3 hours (b), 1 day (c), 3 days (d).

30

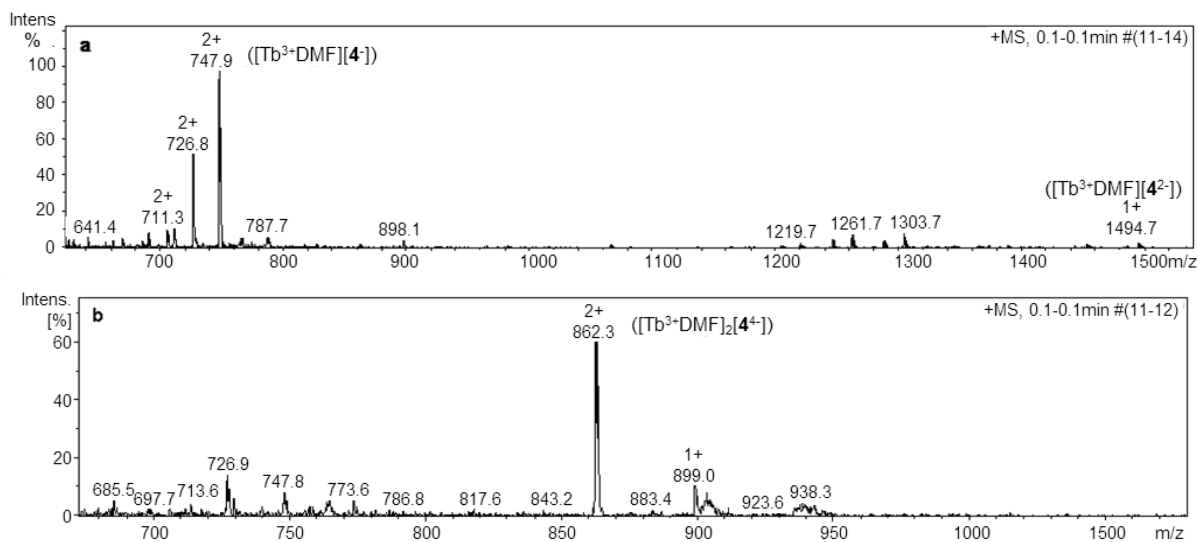


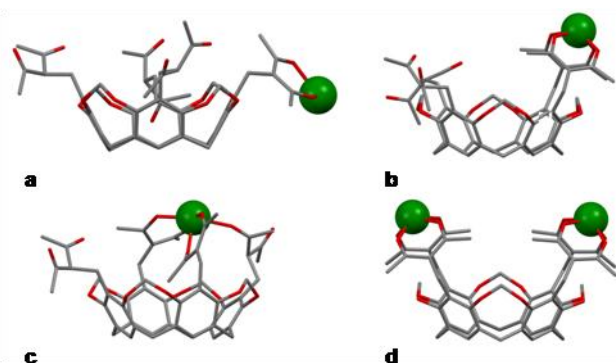
Fig. 4 ESI mass spectra of DMF solutions of **4**, Tb(III) and TEA in 1:1:4 (Tb:4:TEA) concentration ratio recorded within one hour (a) and one day (b) after the preparation of the solutions.

35

Cite this: DOI: 10.1039/c0xx00000x

www.rsc.org/xxxxxx

ARTICLE TYPE



Scheme 2 Possible modes of binding of Tb(III) cations to molecule **4** (lower rim alkyl substituents are omitted). The structures are obtained after PM6 optimization of starting structures built on the basis of present single-crystal X-ray data for molecule **4** (for details see subsection 'Quantum-chemical computations').

The Scheme 2 represents the modes of coordination of Tb(III) ions with **4** via one and two diketonate groups in accordance with the stoichiometries revealed from ESI (Fig. 4) and UV-Vis (Fig.3) spectral data. The coordination of the solvent (DMF) molecules to Tb(III) ions bound with one or two diketonate groups of **4** is rather anticipated due to the high coordination number of Tb(III), although the inclusion of DMF molecules into the cavities of the ligand (Fig. 1 exemplifies this possibility for DMSO) may be another reason.

The above mentioned results indicate the difference between kinetically and thermodynamically favorable modes of the complex formation, which in turn raises the question about the reason of this difference. The UV-Vis and ESI results point to the coordination modes presented in Scheme 2a-c as kinetically favorable, while the structure presented in Scheme 2d can be regarded as thermodynamically favorable. This transformation indicates the time dependent participation of the 1,3-diketonate groups in Tb(III) coordination, which in turn can result from the slowed down keto-enol transformation. Nevertheless the aggregation of the ligand or its complexes with Tb(III) of definite stoichiometry, as well as the hydrolysis of the Tb(III) ions could be considered as possible reasons of the time dependent complex formation.

NMR spectroscopy is a powerful tool to reveal the intermolecular interactions of both the ligand and its complexes in solutions. The aggregation of **4** in both neutral and alkaline conditions (four fold excess of TEA) is insignificant in the DMF-d⁷ solutions (the diffusion constants are presented in Table S2 in ESI). The ¹H NMR spectra of **4** were recorded in DMF-d⁷ at a 4-fold excess of TEA both in the absence and in the presence of Tb(III) salt at 1:1 (Tb:**4**) concentration ratio within one hour after the samples preparation and one day afterwards. The ¹H NMR data reveal a detectable widening of signals corresponding to DMF, TEA and **4** (Fig. S5 in ESI). This tendency may arise from the decreased diffusion of the complexes due to their aggregation in time or the exchange between different structures of complexes. The

diffusion coefficients (Table S2 in ESI) indicate an insignificant aggregation independently on the time after the sample preparation.

It is well known that spin-lattice relaxation times (T_1) are greatly affected by the proximity of the protons to paramagnetic Tb(III) ions and this can be used to obtain valuable information on the intermolecular interactions and structure of the corresponding complexes. Thus the proton spin-lattice relaxation times of all components of the solutions (**4**, DMF and TEA) were measured at various time intervals after the samples preparation. The obtained results (Table 1) reveal the shortening of spin-lattice relaxation times for DMF and TEA molecules within one hour after the sample preparation, which arises from a proximity of the molecules to the Tb(III) ions in these time conditions. These values tend to increase about one order of magnitude after one day storage of the sample (Table 1). This tendency indicates that the storage of the sample results in a displacement of both DMF and TEA molecules from their locations in a close proximity to the Tb(III) ions, which in turn points to time induced complex transformations. These transformations can be assumed on the basis of diverse coordination modes represented in Scheme 2. Indeed, transformation of the coordination modes represented in Scheme 2a,b to those introduced in Scheme 2c,d should be followed by the displacement of both DMF molecules from the inner sphere of Tb(III) ions and triethylammonium (TEAH⁺) ions bound to the diketonate groups. It is worth noting that the above mentioned transformations are in good agreement with the change of the complex stoichiometries revealed from UV-Vis and ESI data (Figs. 3,4).

Table 1 Proton spin lattice relaxation times in DMF-d⁷ solutions of **4** (4.5 mM), Tb(III) and TEA at 1:1:4 concentration ratio were measured under 1 hour and 1 day after their preparation. The numbering of protons corresponds to the assignments in Scheme 1.

Moiety/molecule	T_1 , s	
	One hour	One day
CH ₃ /DMF	0.48	5.98
H ₂ O	0.76	0.78
CH ₃ /TEA	0.73	1.54
CH ₂ /TEA	0.16	1.23
H(1)/ 4	0.93	1.51
H(9) equatorial/ 4	0.49	0.58
H(9) axial/ 4	0.34	0.31
H(8)/ 4	0.54	0.62
H(11)/ 4	0.34	0.61

The above mentioned time induced transformations of the Tb(III) complexes should affect Tb(III) centered luminescence in the solutions. The obtained data (Fig. 5, Table 2) indicate that **4** in basic DMF solutions provides a significant antennae effect on Tb(III) centered luminescence resulting from complex formation. The three bands at 490, 545 and 590 nm in the luminescence

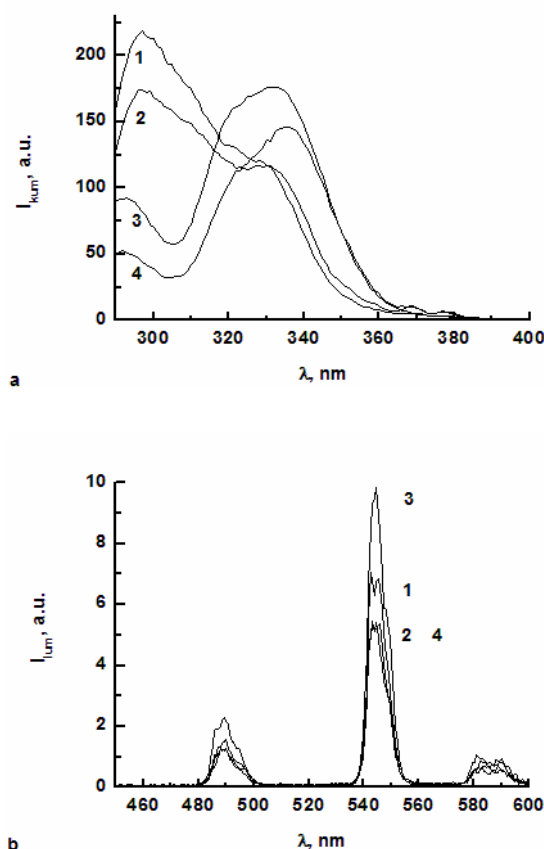


Fig. 5 The excitation (a) and emission (b) spectra for the concentration ratio Tb:4:TEA 1:1:4 (1 and 3 curves) and 2:1:4 (2 and 4 curves) in DMF: immediately (1 and 2 curves) and after 1 day (3 and 4 curves). $C_4=0.45$ mM.

spectra of Tb(III) ions in alkaline DMF solutions of **4** (Fig. 5b) are assigned to $^5D_4-^7F_6$, $^5D_4-^7F_5$ and $^5D_4-^7F_4$ transitions correspondingly. Table 2 presents the intensity of the band at 545 nm, which is the main band of Tb(III) centered luminescence and the corresponding lifetimes of the excited state measured in alkaline DMF solutions at 1:1, 1:2 and 2:1 (Tb:4) concentration ratios under various time conditions. The sensitizing of Tb(III)-centered luminescence occurs within several minutes upon mixing the Tb(III) salt with **4** and TEA in both DMSO and DMF solutions. The corresponding excitation and emission spectra are exemplified for a 1:1:4 (Tb:4:TEA) concentration ratio in DMF solutions (Fig. 5, Table 2).

The obtained results (Fig. 5, Table 2) show a detectable change in time of both the excitation and Tb-centered luminescence spectra. The excitation spectra tend to decrease in intensity at 300-310 nm with a simultaneous increase at 320-350 nm with time (Fig. 5a), which is in good agreement with the changes in the electronic absorption spectra (Fig. 3). The intensities of the steady state luminescence increase in time, although this increase disagrees with the changes in the lifetime values (Table 2). This fact indicates an increased amount of the luminescent complexes in time, although these transformations lower the antennae effect of the ligand or increase the contribution of a radiationless decay. The antennae effect of the ligand should be the largest in the complex with 1:2 stoichiometry. The experimental results indicate no significant difference between the steady state and

time resolved luminescence at 1:1 and 1:2 (Tb:4) concentration ratio, which can be regarded as the indication that the 1:1 stoichiometry is optimal for efficient Tb(III)-centered luminescence. Taking into account the impact of the solvent molecules coordinated with Tb(III) ion to the radiationless decay, the latter contribution should be different for the diverse coordination modes represented in Schemes 2a-d. From this point of view the lifetimes of the excited state (τ) values should be greater for the coordination mode presented in Scheme 2c than those introduced in Schemes 2b,d. Thus, a 1:1 complex with the Tb(III) ion coordinated via two diketonate and one diketone groups (Scheme 2c) and its further transformation into 1:1 and 2:1 complexes (Schemes 2b,d) can be assumed as the reason of the time induced spectral changes. The increase of the Tb(III) concentration on going from 1:1 (Tb:4) to 2:1 concentration ratios (Fig. 5b, Table 2) does not enhance the corresponding intensities and lifetimes of Tb(III) centered emission. Moreover the time resolved changes in the luminescence intensity are less enhanced at 2:1 concentration ratio (Fig. 5b, Table 2), thus confirming the growing extent of 2:1 complexes as the reason of the observed time induced spectral changes. This assumption is in good agreement with ESI spectrometry results (Fig. 4).

Summarizing this issue, it can be concluded that the self-aggregation of **4** or its complexes with Tb(III) should be excluded as the reason of the time dependent complex formation. The hydrolysis of Tb(III) ions can not be excluded in these solutions, although the τ -values are the highest immediately after the solution preparation. This fact disagrees with the transformation from hydroxy- to diketonate complexes as the reason of the changes in time. This in turn points to the slowed down keto-enol conversion as the reason of the long equilibration time for the complex formation of **4** with Tb(III) ions in basic DMF solutions. The excitation of anion ligands to their first singlet excited energy levels, with further energy transfers to the first triplet excited energy levels and then to the excited energy levels of lanthanide ions is well documented as a common mechanisms of energy transfer in lanthanide complexes with 1,3-diketones. The effect of

Table 2 The intensities of the main band at 545 nm (I, a.u.) and lifetimes of the excited state (τ , ms) of Tb(III) centered luminescence in various concentration conditions (designated by Tb(III) concentration (C_{Tb}) and Tb:4:TEA concentration ratio) in DMF solutions at various excitation wavelengths (λ_{ex}) and time intervals (10 minutes and 1 day) between the preparation and measurement of the solutions.

C_{Tb} Tb:4:TEA	λ_{ex} , nm	I, a.u. 10 minutes	I, a.u. 1 day	τ , ms 10 minutes	τ , ms 1 day
0.45 mM 1:2:4	310	88±3	65±2	0.78±0.02	0.51±0.01
	320	99±5	104±4	0.57±0.01	0.43±0.01
	330	136±4	194±5	0.43±0.01	0.29±0.01
0.45 mM 1:1:3	310	100±5	74±2	0.86±0.02	0.48±0.01
	320	88±3	91±3	0.56±0.01	0.36±0.01
	330	84±3	126±4	0.37±0.01	0.23±0.01
0.45 mM 1:1:4	310	71±5	86±2	0.76±0.02	0.46±0.02
	320	70±4	98±4	0.53±0.01	0.34±0.01
	330	81±2	136±5	0.34±0.02	0.20±0.01
0.9 mM 2:1:3	310	72±2	43±2	0.85±0.02	0.45±0.02
	320	67±3	43±2	0.59±0.01	0.33±0.01
	330	73±2	78±3	0.40±0.01	0.21±0.01
0.9 mM 2:1:4	310	54±2	47±2	0.80±0.02	0.48±0.01
	320	53±2	54±3	0.56±0.01	0.34±0.01
	330	69±3	90±4	0.37±0.01	0.22±0.01

the calix[4]resorcinarene backbone consisting of four resorcinol rings with $\pi \rightarrow \pi^*$ transitions in the structure of **4** on the energy transfer mechanism will be highlighted in details in the nearest future and published elsewhere.

5 Hydrophilic colloids with Tb(III)-centered luminescence

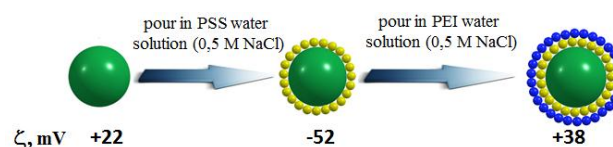
The reprecipitation of the complexes from organic to aqueous solutions with further coating of the nanoparticles by a polyelectrolyte layer provides a synthetic route to get luminescent nanoparticles. The above mentioned results indicate the coexistence of 1:1 and 2:1 complexes in solutions as the reason restricting their separation. The water insolubility of the Tb(III) complexes is the key factor affecting their reprecipitation from organic to aqueous solutions. Thus the reprecipitation procedure is a route to convert complexes insoluble in water together with “free” ligand into colloids, while the water soluble Tb(III) ions or their hydroxy-forms together with both TEA and [TEAH]⁺ can be easily separated from the hard colloids by a phase separation. In order to minimize the contribution of the “free” ligand the reprecipitation has been performed for the solutions with 1:1 and 2:1 (Tb:4) concentration ratio.

The nature of the organic solvent together with the concentration and time conditions were varied in order to optimize the synthetic conditions of the reprecipitation procedure. The DMF solutions of the luminescent complexes provide a better basis for further reprecipitation than the ones based on DMSO from the viewpoint of the averaged diameter (d) and polydispersity indices (PDI), which are presented in Table 3 and Table S3 in ESI for DMF and DMSO solutions correspondingly. The reprecipitation without polyelectrolyte coating reveals positively charged colloids, where the electrokinetic potential is +22mV, d and PDI are 1170 nm and 0.72, correspondingly. These colloids tend to aggregate and precipitate within a short period of time. This fact reveals a negatively charged polyelectrolyte as the most appropriate first layer. Indeed the efficient adsorption and self-assembly of poly(sodium 4-styrenesulfonate) (PSS) is evident from the recharging of the colloids (Table 3). The layer-by-layer polyelectrolyte deposition on the positively charged luminescent core is represented in Scheme 3. It is worth noting that the time duration from the preparation of the complexes in DMF solutions and their reprecipitation affects the size and PDI values of the colloids. Both values tend to decrease, when the reprecipitation is performed after the storage of the solution. In particular the size and PDI values of the colloids are the best when the interval between the organic solution preparation and its reprecipitation to the aqueous PSS solution is about one day (Table 3). Moreover, storage of the colloids made from recently prepared solutions results in changes of the colloid characteristics (Table 3), while the similar data for PSS-coated colloids made from the solutions after one day storage tend to remain constant for one week at least. The specified stability of the colloids in time is in good agreement with the tendency highlighted by Sukhishvili⁴³ that the exchange between polyelectrolytes within the multilayer and those in the solutions is slowed down, which in turn restricts the

degradation of the layer-by-layer deposition from the oppositely charged polyelectrolytes.

Table 3. The averaged sizes (d, nm), PDI and electrokinetic potential (ζ , mV) of the PSS- and PSS-PEI-coated colloids reprecipitated from the DMF solutions at 1:1:4 (Tb:4:TEA) concentration ratio after various time intervals from the preparing of the solutions to their reprecipitation (time 1) and various duration of the storage of the colloids (time 2).

time 1	time 2	layer	d, nm	PDI	ζ , mV
10 minutes	1 day	PSS	348±5	0.74	-52±3
		PSS-PEI	310±7	0.61	+38±2
	3 days	PSS	105±2	0.33	-42±2
		PSS-PEI	103±3	0.31	+38±2
	7 days	PSS	80±3	0.41	-38±4
		PSS-PEI	65±2	0.41	+38±3
3 hours	1-7 days	PSS	142±2	0.22	-51±2
		PSS-PEI	195±5	0.27	+34±3
1 day	1-7 days	PSS	160±5	0.12	-55±3
		PSS-PEI	197±7	0.18	+39±2
3 days	1-7 days	PSS	141±5	0.17	-46±3
		PSS-PEI	211±6	0.30	+41±2



Scheme 3 Schematic presentation of layer-by-layer deposition of PSS and PEI on the luminescent core.

The AFM image and the size distribution exemplified for the dried samples of the PSS-PEI-coated colloids on a mica surface (Fig.S7 in ESI) reveals the less size (30-40 nm) than the DLS results (103±3nm, Table 3). This deviation results from the difference between the size of the hydrated shells in solution and the solid cores, which are revealed in the dried samples.

It is well known that the luminescence properties of core-shell colloids depend on both the nature of the luminophores within the cores and the colloid characteristics, such as size and aggregation behavior. The luminescence characteristics of the colloids made from the DMF solutions at 1:1:4 (Tb:4:TEA) concentration ratio depend on the time interval between the preparation and reprecipitation of the solutions (Table 4). This dependence indicates that the content of the reprecipitated luminescent core is influenced by the time intervals. The changes in time observed for the colloids made from the recently prepared solutions (Tables 3,4) most probably result from the slowed down transformations of the complexes similar with those taking part in solutions (Table 2). The presented data show that a time interval of one day is optimal for the synthesis of the colloids. The coating of PSS-deposited colloids by polyethyleneimine (PEI) results in the recharging from negative to positive (Table 3), while the sizes and the luminescence characteristics for PSS- and PSS-PEI-coated colloids are rather similar (Tables 3,4).

Cite this: DOI: 10.1039/c0xx00000x

www.rsc.org/xxxxxxx

ARTICLE TYPE

Table 4 The intensities of the main band at 545 nm (I , a.u.) and lifetimes of the excited state (τ , ms) of Tb(III) centered luminescence of the colloids made from the DMF solutions at 1:1:4 (Tb:4:TEA) concentration ratio at various excitation wavelengths (λ_{exc}) and time intervals (10 minutes, 3 hours and 1 day) between the preparation of the DMF solutions and their reprecipitation into the aqueous ones.

layer	λ_{exc} , nm	I , a.u. 10 minutes	I , a.u. 3 hours	I , a.u. 1 day	τ , ms 10 minutes	τ , ms 3 hours	τ , ms 1 day
PSS	310	81±3	319±6	548±8	0.29±0.01*	0.28±0.01*	0.27±0.02*
	320	95±5	349±6	643±8	0.28±0.01	0.22±0.01	0.26±0.01
	330	90±4	320±6	689±9	0.27±0.01	0.24±0.02	0.25±0.01
PSS-PEI	310	80±4	180±6	436±7	0.28±0.01	0.19±0.01	0.29±0.02
	320	91±3	181±5	528±6	0.28±0.02	0.22±0.02	0.29±0.02
	330	94±5	293±6	516±5	0.27±0.01	0.22±0.02	0.29±0.02

* these values remain unchanged within 8 days.

5 The time resolved luminescence data reveal no degradation of the luminescent complexes in the core within one week at least (Table 4). The steady state luminescence also tends to remain on a convenient level within at least one week, which is no less of a half of the initial intensity (Fig. 6a). Moreover, no more or less significant degradation of the luminescence occurs in the commonly applied buffer systems, such as citrate, phosphate buffers and Tris, which is exemplified by the I/I_0 values in Fig. 6b, where I_0 and I are the intensities of the main band in water and in the buffer solutions correspondingly.

time of their storage: within 1 day (1); 4 days (2); 9 days (3), $\lambda_{\text{exc}}=310$ nm. (b) The I/I_0 values in PSS- (1,3,5) and PEI-PSS- coated (2,4,6) colloids at various concentrations of buffers: 1,2 - monosodium citrate/sodium hydroxide (pH 6.0); 3,4 - monopotassium dihydrogen phosphate/disodium hydrogen phosphate (pH 6.2); 5,6 - Tris (pH 7.0). The concentration of colloids is $2.0 \text{ g}\cdot\text{L}^{-1}$, $C_{\text{Tb(III)}}=0.75 \text{ mM}$.

Conclusions

25 The new synthesized calix[4]resorcinarene cavitand with four 1,3-diketone groups fixed at the upper rim is introduced in the present work as a ligand for Tb(III) ions. The ^1H NMR spectroscopy results indicate restricted keto-enol conversion due to the steric hindrance of the methylenedioxy groups, which is the reason of the increased equilibration time of the complex formation in DMSO and DMF solutions in the presence of triethylamine and $\text{Tb}(\text{NO}_3)_3$. This tendency is shown from the time induced spectral changes. Moreover, the Job plot analysis of the electronic absorption data reveals the different stoichiometry of kinetically and thermodynamically favorable complex forms, which is confirmed by ESI mass spectrometry data. The fluorescence data show a significant antennae effect of the cavitand on the Tb(III) centered luminescence, although the interference of complex forms with diverse stoichiometry restricts their separation. The work introduces a facile synthetic route to convert luminescent complexes into hydrophilic nanosized colloids through the reprecipitation from organic to aqueous solutions with additional polyelectrolyte deposition. The luminescence and colloid properties of the synthesized hydrophilic colloids in aqueous solutions remain unchanged within one week at least with no degradation of the luminescence in commonly applied buffer solutions.

Experimental section

Reagents and materials

50 Terbium(III) nitrate hydrate ($\text{Tb}(\text{NO}_3)_3\cdot x\text{H}_2\text{O}$), (Alfa Aesar), triethylamine (TEA), (Acros Organics), poly(sodium 4-styrenesulfonate) (PSS) ($MW_{\text{average}}=70\ 000$) (Acros Organics), polyethyleneimine (PEI) branched ($MW_{\text{average}}=25\ 000$) (Aldrich Chemistry), potassium dihydrogen phosphate (AppliChem), disodium hydrogen phosphate (Acros Organics), citric

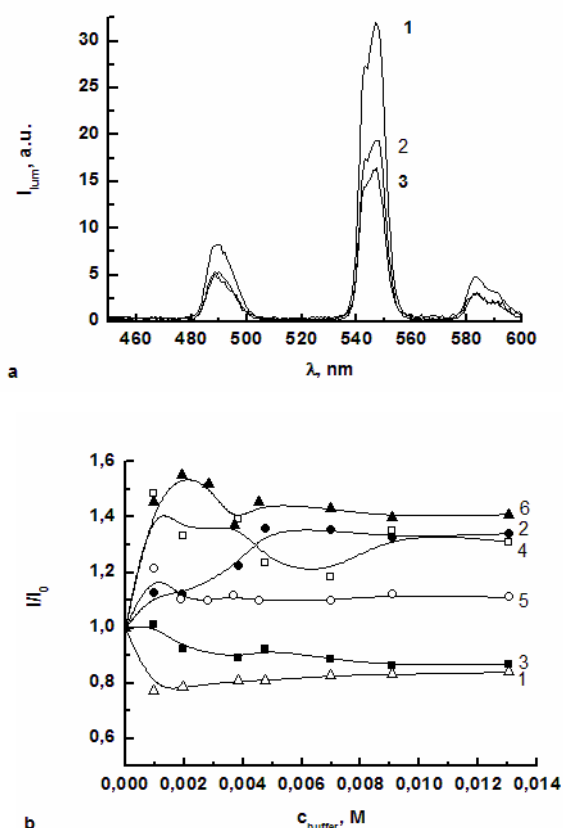


Fig. 6 (a) The luminescence spectra of the PSS-coated colloids reprecipitated from 1:1:4 (Tb:4:TEA) DMF solutions under the various

acid/sodium hydroxide solution pH 6.0 (Fluka), tris(hydroxymethyl)aminomethane (Tris) (Acros Organics) were used as commercially received without further purification. N,N-Dimethylformamide (DMF) (Acros Organics) and dimethyl sulfoxide (DMSO) (Acros Organics) were distilled over P₂O₅ and KOH apparently. CDCl₃ (99.8% isotopic purity) and DMF-d₇ (99.5% isotopic purity) from Aldrich were used for NMR spectroscopy measurements.

Synthesis

The synthetic route, the structural formulae and numbering of atoms of the compound are shown in Scheme 1. The calix[4]resorcinarene **1**⁴¹, and the tetrakis(methyl)- and tetrakis(bromomethyl)- calix[4]resorcinarene derived cavitands **2** and **3**⁴² were obtained as described earlier.

15 Synthesis of 7,11,15,28-tetrakis-[(acetylaceton-3-yl)methyl]-1,21,23,25-tetrapentyl-2,20:3,19-dimetheno-1H,21H,23H,25H-bis[1,3]dioxocino[5,4-i:5',4'-i']benzo(1,2-d:5,4-d')bis[1,3]benzodioxocin stereoisomer (cavitand **4**)

A mixture of the sodium salt of acetylacetonone (NaAA) (2.93 g, 24 mmol) and tetrakis(bromomethyl)cavitand **3** (4.76 g, 4 mmol) in anhydrous dioxane (100 mL) was refluxed with stirring for 17 h under argon. The reaction mixture was filtered and the solvent was distilled off from the filtrate *in vacuo*. The residue was acidified by 1M HCl (100 ml). After addition of CH₂Cl₂ (100 ml) the mixture was vigorously stirred. The organic layer was separated, washed three times with water, dried with MgSO₄ and concentrated. Solvent residues were removed at 80°C *in vacuo*. After recrystallization of crude product (4.74 g) from a mixture of ethanol-chloroform (10:1) a pale yellow powder of **4** was obtained (3.2 g) in 63% yield. Mp.128-132 °C. ¹H NMR (600.13 MHz, CDCl₃, 303 K, ppm), δ 16.75-16.85 (m, OH_{en}), 6.92-7.00 (m, 4H, H(8)), 5.78_{en}, 5.76_{ket} (d, ²J_{en} = 6.2 Hz, ²J_{ket} = 6.6 Hz, 4H, H(9)_{out}), 4.64-4.70 (m, 4H, H(10)), 4.31_{en}, 4.19_{ket}, (d, ²J_{en} = 6.2 Hz, ²J_{ket} = 6.6 Hz, 4H, H(9)_{in}), 3.88 (t, ³J = 5.5 Hz, 4H for keto form, H(3)_{ket}), 3.42 (s, H(4)_{en}) and 2.82 (d, ³J_{ket} = 5.5 Hz H(4)_{ket}) (8H, H(4)), 2.0-2.2 (m, 24H, H(1) and 8H, H(11)), 1.25-1.45 (m, 24H, H(12), CH₂), 0.92, 0.86 (t, ³J = 5.5 Hz, 12H, H(13)). ¹³C NMR (150.9 MHz, CDCl₃, 303 K, ppm), δ, keto form: 203.9 C(2); 153.3 C(6); 138.3 C(7); 125.1 C(5); 119.2 C(8); 98.9 C(9); 67.6 C(3); 37.0 C(10); 31.0 C(11); 32.0, 30.1, 23.6 C(12); 29.6 C(1); 14.2 C(13); 22.8 C(4); enol form: 191.3 C(2); 108.4 C(3); 100 C(9); 23.5 C(4). IR (nujol, cm⁻¹): ν = 3404 (overtone ν(C=O)); 3000-2800 (ν(CH), ν(CH₂) and ν(CH₃) for KBr pellet); 1725, 1701 (ν(C=O)); 1588, 1466 (νPh), 1377, 1358, 1306, 1236, 1149 (ν_{as}(CCC)); 1077, 1017, 981 (ν_s(CCC)). MALDI-MS (*m/z*): calcd for C₇₆H₉₆O₁₆ [M + Na]⁺ 1287.6591, found: 1287.6596. Calcd for C₇₆H₉₆O₁₆: C, 72.13; H, 7.65. Found: C, 71.85; H, 7.87.

Synthesis of the colloids

DMF solutions at various Tb:4:TEA concentration ratio and the concentration of **4** of 22.5 mM were added dropwise to water solution of PSS (1g·L⁻¹) and NaCl (0.5 M) at pH=6.0 under intensive stirring (1250 rpm). The volume ratio of the DMF to aqueous solutions was 1:5. After the addition the dispersion was exposed to ultrasonication for 30 minutes.

To synthesize PSS-PEI-coated colloids, the PSS-coated dispersion was centrifuged (11 000 rpm, 15 minutes). The supernatant was poured out, the solution of PEI (1g·L⁻¹) and NaCl (0.5 M) at pH 7.0 was added to the precipitate. Then the

dispersion was exposed to ultrasonication for 30 minutes.

The synthesis of the PSS-PEI-PSS-coated colloids was performed through the precipitation and further addition of the PSS aqueous solution.

The PSS-, PSS-PEI- and PSS-PEI-PSS-coated colloid were diluted to adjust the concentration of nanoparticles to 2.0 g·L⁻¹ level through the addition of 0.5 ml of the colloids to 4.5 ml of twice distilled water prior filtered through a PVDF membrane using a Syringe Filter (0.45 μm).

Colloids have been ultrasonicated for 30 min before measurements. All measurements have been performed at least three times.

Methods

Microanalyses of C, H, and N were carried out with a CHN-3 analyser. Melting points of compounds were measured with a Boetius hotstage apparatus. Mass spectra (MALDI) were detected on a Bruker Ultraflex III MALDI-TOF/TOF mass spectrometer.

NMR experiments were performed on a Bruker AVANCE-600 spectrometer at 303K equipped with a 5 mm diameter broadband probe head working at 600.13 MHz in ¹H and 150.864 MHz in ¹³C experiments. Chemical shifts in ¹H and ¹³C spectra were reported relative to the solvent as internal standard (CDCl₃ δ(¹H) 7.27 ppm, δ(¹³C) 77.2 ppm; DMF δ(¹H) 2.9 ppm). The spectrometer AVANCE-600 was equipped with a multinuclear z-gradient inverse probe head capable of producing gradients with strength of 50 G cm⁻¹. The Fourier transform pulsed-gradient spin-echo (FT-PGSE) experiments⁴⁴⁻⁴⁶ were performed by BPP-STE-LED (bipolar pulse pair-stimulated echo-longitudinal eddy current delay) sequence.⁴⁷ Data were acquired with a 30.0-50.0 ms diffusion delay, with bipolar gradient pulse duration from 3.4 to 4.0 ms (depending on the system under investigation), 1.1 ms spoil gradient pulse (30%) and a 5.0 ms eddy current delay. The bipolar pulse gradient strength was varied incrementally from 0.01 to 0.32 T/m in 16 steps. The temperature was set and controlled at 303K with a 535 l/h airflow rate in order to avoid any temperature fluctuations owing to sample heating during the magnetic field pulse gradients. The T1 times were measured using the inverse-recovery pulse sequence.

The X-ray diffraction data for 4·2DMSO were collected on a Bruker Smart APEX II CCD diffractometer using graphite monochromated Mo Kα (λ = 0.71073 Å) radiation at 296(2)K.

The structure was solved by direct method using the SHELXS⁴⁸ program and refined by the full matrix least-squares using SHELXL⁴⁸ programs. All non-hydrogen atoms were refined anisotropically. Hydrogen atoms were placed on the calculated positions and were refined as riding atoms. All calculations were performed on a PC using the WinGX⁴⁹ series of programs. Analysis of the intermolecular interactions was performed using the program PLATON.⁵⁰ The Mercury⁵¹ program package was used for the preparation of the Figures. Brief crystallographic information is given in Table 1. Crystallographic data (except structure factors) for 4·2DMSO were deposited in the Cambridge Crystallographic Data Centre with supplementary publication number CCDC 995107. Copies of these data can be obtained upon free of charge application to the CCDC (12 Union Road, Cambridge CB2 1EZ, UK. Fax: (internat.) + 44 1223/336 033; E-mail: deposit@ccdc.cam.ac.uk).

The dynamic light scattering (DLS) measurements were

performed by means of the Malvern Mastersize 2000 particle analyzer. A He-Ne laser operating at 633 nm wavelength and emitting vertically polarized light was used as a light source. The measured autocorrelation functions were analyzed by Malvern DTS software and the second-order cumulant expansion methods. The effective hydrodynamic radius (R_H) was calculated by the Einstein-Stokes relation from the first cumulant: $D = k_B T / 6\pi\eta R_H$, where D is the diffusion coefficient, k_B is the Boltzmann constant, T is the absolute temperature, and η is the viscosity. The diffusion coefficient was measured at least three times for each sample. The average error in these experiments is approximately 4%. Zeta potential “Nano-ZS” (MALVERN) using laser Doppler velocimetry and phase analysis light scattering was used for zeta potential measurements.

An atomic force microscope (MultiMode V, USA) has been used to reveal the morphology of the nanoparticles modified by surfactants. The 250-350 kHz cantilevers (Veeco, USA) with silicone tips (tip curvature radius is of 10-13 nm) have been used in all measurements. The microscopic images have been obtained by means of 8279JV scanner with 256×256 resolution. The scanning rate was 1 Hz. The antivibrational system (SG0508) has been used to eliminate external distortions. The tip-convolution effect has been minimized by processing the obtained AFM data with the use of the software (WSxM 5.0, Zod 2.0 and MatLAB). The calibration has been performed by the use of imaging special calibration grid (STR3-1800P, VLSI Standards Inc.) in the temperature range 20-60 °C.

The aqueous dispersions of nanoparticles (0.484 g L⁻¹) have been ultrasonicated within 30 minutes and then the droplet of the sample has been placed on mica surface with the roughness no more than 1-5 nm. The AFM imaging has been performed after water evaporation.

The steady-state luminescence spectra were recorded on a spectrofluorometer FL3-221-NIR (Jobin Yvon) with SPEX FL-1042 phosphorimeter in 10 mm quartz cuvettes. Excitation of samples was performed at 310, 320, 330 nm, and emission detected at 545 nm with 1 nm slit width for both excitation and emission. Time-resolved measurements were performed using the following parameters: time per flash-49.00 ms, flash count-200 ms, initial delay-0.05 ms and sample window-2 ms. The normalized fluorescence decay curves are presented in Fig.S8 in ESI.

Quantum-chemical computations. Structural modeling of complexes was performed with the use of MOPAC 2009 software.⁵² The PM6 semiempirical method was applied,⁵³ which allowed to minimize computational time and resources and to maintain the accuracy comparable to non-empirical approaches. Further simplification of the computations was achieved by replacement of Tb(III) ion by its closed-shell analogy – Lu(III) ion. Such a replacement was a reasonable approximation as the geometry of lutetium complexes is usually close to the corresponding related complexes of terbium.⁵⁴

Notes and references

^a A. E. Arbuзов Institute of Organic and Physical Chemistry, Kazan Scientific Center of Russian Academy of Sciences, Arbuzov str., 8, 420088, Kazan, Russia

^b Kazan Federal University, Kremlevskaya str., 18, 420008, Kazan, Russia

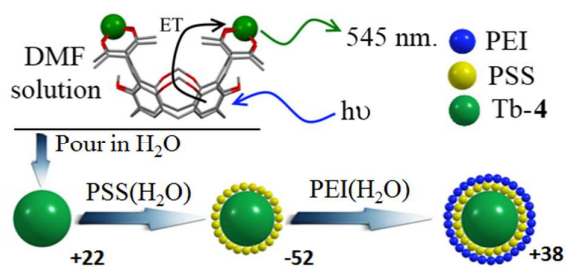
^c Zavoisky Physical-Technical Institute of Kazan Scientific Center of Russian Academy of Sciences, Sibirsky tract, 10/7, 420029, Kazan, Russia

^d Department of Chemistry, KU Leuven, Celestijnenlaan 200F, 3001 Leuven, Belgium

† Electronic Supplementary Information (ESI) available: [details of any supplementary information available should be included here]. See DOI: 10.1039/b000000x/

1. S. Comby, E. M. Surender, O. Kotova, L. K. Truman, J. K. Molloy, T. Gunnlaugsson, *Inorg. Chem.*, 2014, **53**, 1867.
2. M. C. Heffern, L. M. Matosziuk, T. J. Meade, *Chem. Rev.*, DOI: 10.1021/cr400477t.
3. J.-C.G. Bünzli, *Chem. Rev.*, 2010, **110**, 2729.
4. T. Gunnlaugsson, M. Glynn, G. M. Tocci, P. E. Kruger, F. M. Pfeffer, *Coord. Chem. Rev.*, 2006, **250**, 3094.
5. J. L. Worlinsky, S. Basu, *J. Phys. Chem. B*, 2009, **113**, 865.
6. R. Huttunen, Shweta, E. Martikkala, M. Lahdenranta, P. Virta, P. Hänninen, H. Härmä, *Analytical Biochemistry*, 2011, **415**, 27.
7. C. S. Bonnet, M. Devocellec, T. Gunnlaugsson, *Org. Biomol. Chem.*, 2012, **10**, 126.
8. M. Karbowiak, J. Cichos, K. Buczek, *J. Phys. Chem. B*, 2014, **118**, 226.
9. C. Freund, W. Porzio, U. Giovannella, F. Vignali, M. Pasini, S. Destri, A. Mech, S. Di Pietro, L. Di Bari, P. Mineo, *Inorg. Chem.*, 2011, **50**, 5417.
10. S. Gago, J. A. Fernandes, J. P. Rainho, R. A. Sá Ferreira, M. Pillinger, A. A. Valente, T. M. Santos, L. D. Carlos, P. J. A. Ribeiro-Claro, I. S. Gonçálves, *Chem. Mater.*, 2005, **17**, 5077.
11. A. P. Bassett, S. W. Magennis, P. B. Glover, D. J. Lewis, N. Spencer, S. Parsons, R. M. Williams, L. De Cola, Z. Pikramenou, *J. Am. Chem. Soc.*, 2004, **126**, 9413.
12. J. Yuasa, T. Ohno, K. Miyata, H. Tsumatori, Y. Hasegawa, T. Kawai, *J. Am. Chem. Soc.*, 2011, **133**, 9892.
13. Y.-M. Luo, Z. Chen, R.-R. Tang, L.-X. Xiao, H.-J. Peng, *Spectrochimica Acta Part A*, 2008, **69**, 513.
14. J. Shi, Y. Hou, W. Chu, X. Shi, H. Gu, B. Wang, Z. Sun, *Inorg. Chem.*, 2013, **52**, 5013.
15. J.-C. G. Bünzli, *Chem. Rev.*, 2010, **110**, 2729.
16. C.-J. Xu, B.-G. Li, J.-T. Wan, Z.-Y. Bu, *Spectrochimica Acta Part A*, 2011, **82**, 159.
17. B. S. Creaven, D. F. Donlon, J. McGinley, *Coordination Chemistry Reviews*, 2009, **253**, 893.
18. D. T. Schuhle, J. A. Petersa, J. Schatz, *Coordination Chemistry Reviews*, 2011, **255**, 2727.
19. N. Iki, *Supramolecular Chemistry*, 2011, **23**, 160.
20. N. Iki, T. Horiuchi, H. Oka, K. Koyama, N. Morohashi, C. Kabuto, S. Miyano, *J. Chem. Soc. Perkin Trans.* 2001, **2**, 2219.
21. N. Iki, S. Hiro-Oka, T. Tanaka, C. Kabuto, H. Hoshino, *Inorg. Chem.*, 2012, **51**, 1648.
22. A. R. Mustafina, S. V. Fedorenko, O. D. Konovalova, A. Yu. Menshikova, N. N. Shevchenko, S. E. Soloveva, A. I. Konovalov, I. S. Antipin, *Langmuir*, 2009, **25**, 3146.
23. S. V. Fedorenko, O. D. Bochkova, A. R. Mustafina, V. A. Burilov, M. K. Kadirov, C. V. Holin, I. R. Nizameev, V. V. Skripacheva, A. Yu. Menshikova, I. S. Antipin, A. I. Konovalov, *J. Phys. Chem. C*, 2010, **114**, 6350.
24. H. Härmä, C. Graf, P. Hänninen, *J. Nanopart. Res.*, 2008, **10**, 1221.
25. H. Härmä, L. Dähne, S. Pihlasalo, J. Suojanen, J. Peltonen, P. Hänninen, *Anal. Chem.*, 2008, **80**, 9781.
26. A. Valanne, J. Suojanen, J. Peltonen, T. Soukka, P. Hänninen, H. Härmä, *Analyst*, 2009, **134**, 980.
27. A. Mustafina, R. Zairov, M. Gruner, A. Ibragimova, D. Tatarinov, I. Nizameev, N. Nastapova, V. Yanilkin, M. Kadirov, V. Mironov, A. Konovalov, *Colloids Surf., B*, 2011, **88**, 490.
28. R. Zairov, A. Mustafina, N. Shamsutdinova, M. H. Rummeli, R. Amirov, V. Burilov, M. Pinus, V. Morozov, V. Ivanov, E. Gogolashvili, D. Tatarinov, V. Mironov, A. Konovalov, *Journal of Nanoparticle Research*, 2012, **14**, 1018.

29. N. Davydov, R. Zairov, A. Mustafina, V. Syakayev, D. Tatarinov, V. Mironov, S. Eremin, A. Kononov, M. Mustafin, *Analytica Chimica Acta*, 2013, **784**, 65.
30. C. Spino, L. L. Clouston, D. J. Berg, *Can. J. Chem.*, 1997, **75**, 1047.
31. C. Pettinari, F. Marchetti, A. Drozdov, *Elsevier*, 2003, 97.
32. C. Cativiela, J. L. Serrano, M. M. Zurbano, *J. Org. Chem.* 1995, **60**, 3074.
33. K. Fujimoto, S. Shinkai, *Tetrahedron Letters*, 1994, **35**, 2915.
34. S. N. Podyachev, S. N. Sudakova, A. K. Galiev, A. R. Mustafina, V. V. Syakaev, R. R. Shagidullin, I. Bauer, A. I. Kononov, *Russ. Chem. Bull. Int. Ed.*, 2006, **55**, 2000.
35. K. Nakanishi, *Infrared Absorption Spectroscopy - Practical*, Holden-Day, San Francisco, 1962, pp. 233.
36. L. Sobczyk, S. J. Grabowski, T. M. Krygowski, *Chem. Rev.*, 2005, **105**, 3513.
37. V. Bertolasi, V. Ferretti, P. Gilli, X. Yao, C. Li, *New J. Chem.*, 2008, **32**, 694.
38. J. N. Spencer, E. S. Holmbe, M. R. Kirshenbaum, D. W. Firth, P. B. Pinto, *Can. J. Chem.*, 1982, **60**, 1178.
39. E. Ferrari, M. Saladini, F. Pignedoli, F. Spagnolo, R. Benassi, *New J. Chem.*, 2011, **35**, 2840.
40. D. J. Bray, K. A. Jolliffe, L. F. Lindoy, J. C. McMurtrie, *Tetrahedron*, 2007, **63**, 1953.
41. L. M. Tunstad, J. A. Tucker, E. Dalcanale, J. Weiser, J. A. Bryant, J. C. Sherman, R. C. Helgeson, C. B. Knobler, D. J. Cram, *J. Org. Chem.*, 1989, **54**, 1305.
42. H. Boerrigter, W. Verboom, D. N. Reinhoudt, *J. Org. Chem.*, 1997, **62**, 7148.
43. S. A. Sukhishvili, E. Kharlampieva, V. Izumrudov, *Macromolecules*, 2006, **39**, 8873.
44. P. Stilbs, *Prog. Nucl. Magn. Reson. Spectrosc.*, 1987, **19**, 1.
45. Y. Cohen, L. Avram, L. Frish, *Angew. Chem.*, 2005, **44**, 520.
46. Jr. C. S. Johnson, *Prog. Nucl. Magn. Reson. Spectrosc.* 1999, **34**, 203.
47. D. Wu, A. Chen, Jr. C. S. Johnson, *J. Magn. Reson.*, 1995, **115**, 260.
48. G. M. Sheldrick, *Acta Crystallogr., Sect. A: Found. Crystallogr.*, 2008, **64**, 112.
49. L. J. Farrugia, *J. Appl. Cryst.*, 1999, **32**, 837.
50. A. L. Spek, *J. Appl. Cryst.*, 2003, **36**, 7.
51. (a) I. J. Bruno, J. C. Cole, P. R. Edgington, M. K. Kessler, C. F. Macrae, P. McCabe, J. Pearson, R. Taylor, *Acta Cryst.*, 2002, **58**, 389; (b) C. F. Macrae, P. R. Edgington, P. McCabe, E. Pidcock, G. P. Shields, R. Taylor, M. Towler, J. van de Streek, *J. Appl. Crystallogr.*, 2006, **39**, 453.
52. MOPAC 2009, <http://openmopac.net/MOPAC2009.html>.
53. J. J. P. Stewart, *J. Mol. Modeling*, 2007, **13**, 1173.
54. R. O. Freire, A. M. Simas, *J. Chem. Theory Comput.*, 2010, **6**, 2019.



Luminescent hydrophilic core-shell nanoparticles are synthesized through reprecipitation and polyelectrolyte deposition techniques from Tb(III) complexes of novel tetra-1,3-diketone cavitand.